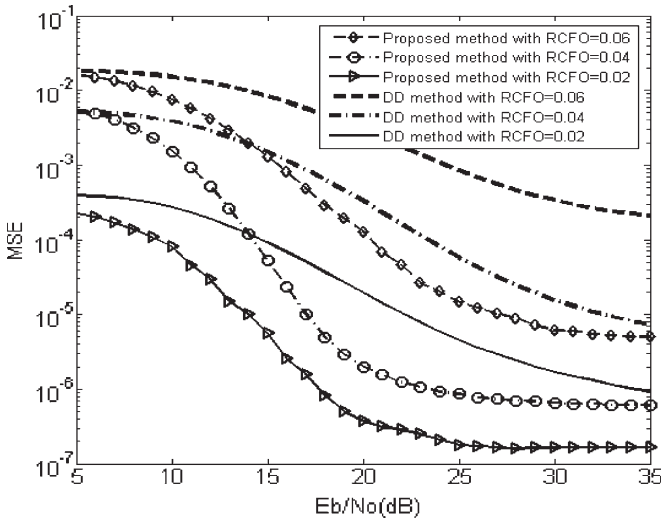

Fig. 2. MSEs of the two methods versus E_b/N_0.

is highly improved compared with the DD algorithm in [9], because the interference introduced by the decision errors on the subchannels is minimized in the proposed method.

VI. Conclusion

We have proposed a new SNR-assisted DD method to estimate the RCFO in wireless OFDM systems, which can greatly reduce the effect of the decision errors on the RCFO estimation. The performance of the proposed method with the optimal SNR threshold is highly improved compared with the conventional DD algorithm. The simulation results indicate that the MSE of the RCFO estimation by the proposed scheme is less than one tenth of that by the DD algorithms with a simple hard decision scheme when the average SNR is greater than 15 dB. It is found that the new estimators yield dramatic performance improvements over the conventional DD estimator at a moderate increase in computational complexity. With very little additional hardware, this new proposed scheme can be implemented in wireless OFDM systems to track the residual frequency offset.

Acknowledgment

The authors would like to thank the reviewers for their comments that led to improvements in this paper.

References

[1] T. Pollet, M. Van Bladel, and M. Moeneclaey, "BER sensitivity of OFDM systems to carrier frequency offset and Wiener phase noise," *IEEE Trans. Commun.*, vol. 43, no. 234, pp. 191–193, Feb.–Apr. 1995.

[2] M. Speth, S. A. Fechtel, G. Fock, and H. Meyr, "Optimum receiver design for wireless broad-band systems using OFDM—Part I," *IEEE Trans. Commun.*, vol. 47, no. 11, pp. 1668–1677, Nov. 1999.

[3] M. Speth, S. A. Fechtel, G. Fock, and H. Meyr, "Optimum receiver design for OFDM-based broadband transmission. II. A case study," *IEEE Trans. Commun.*, vol. 49, no. 4, pp. 571–578, Apr. 2001.

[4] H. Chen and G. J. Pottie, "A comparison of frequency offset tracking algorithms for OFDM," in *Proc. IEEE GLOBECOM*, 2003, pp. 1069–1073.

[5] S. Kapoor, D. J. Marchok, and E.-F. Huang, "Pilot assisted synchronization for wireless OFDM systems over fast time varying fading channels," in *Proc. 48th IEEE VTC*, May 18–21, 1998, vol. 3, pp. 2077–2080.

[6] S.-Y. Liu and J.-W. Chong, "A study of joint tracking algorithms of carrier frequency offset and sampling clock offset for OFDM-based WLANs," in *Proc. IEEE Int. Conf. Commun., Circuits Syst. West Sino Expo.*, Jun. 29–Jul. 1, 2002, vol. 1, pp. 109–113.

[7] W. Lei, J. Lu, and J. Gu, "A new pilot assisted frequency synchronization for wireless OFDM systems," in *Proc. IEEE ICASSP*, Apr. 6–10, 2003, vol. 4, pp. IV-700–IV-703.

[8] N. Lashkarian and S. Kiaei, "Class of cyclic-based estimators for frequency-offset estimation of OFDM systems," *IEEE Trans. Commun.*, vol. 48, no. 12, pp. 2139–2149, Dec. 2000.

[9] K. Shi, E. Serpedin, and P. Ciblat, "Decision-directed fine synchronization in OFDM systems," *IEEE Trans. Commun.*, vol. 53, no. 3, pp. 408–412, Mar. 2005.

[10] S. Boumard, "Novel noise variance and SNR estimation algorithm for wireless MIMO OFDM systems," in *Proc. IEEE GLOBECOM*, Dec. 1–5, 2003, vol. 3, pp. 1330–1334.

[11] X. Xu, Y. Jing, and X. Yu, "Subspace-based noise variance and SNR estimation for OFDM systems," in *Proc. IEEE Mobile Radio Appl. Wireless Commun. Netw. Conf.*, Mar. 13–17, 2005, vol. 1, pp. 23–26.

[12] H. Xu, G. Wei, and J. Zhu, "A novel SNR estimation algorithm for OFDM," in *Proc. 61st IEEE VTC—Spring*, May 30–Jun. 1, 2005, vol. 5, pp. 3068–3071.

[13] R. E. Ziemer and R. L. Peterson, *Introduction to Digital Communication*. Hemel Hempstead, U.K.: Prentice–Hall.

[14] [Online]. Available: www.ieee802.org/16/pub/backgrounder.html

Three-Stage Irregular Convolutional Coded Iterative Center-Shifting K-Best Sphere Detection for Soft-Decision SDMA–OFDM

Li Wang, Lei Xu, Sheng Chen, *Fellow, IEEE*, and Lajos Hanzo, *Fellow, IEEE*

***Abstract*—The iterative exchange of extrinsic information between the K-best sphere detector (SD) and the channel decoder is appealing since it is capable of achieving a near maximum *a posteriori* (MAP) performance at a moderate complexity. However, the computational complexity imposed by the K-best SD significantly increases when using a large value of K for the sake of maintaining a near-MAP performance in a high-throughput uplink spatial-division multiple access (SDMA) orthogonal frequency-division multiplexing (OFDM) system supporting a large number of users and/or a high number of bits/symbol. This problem is further aggravated when the number of users/mobile stations (MSs) U exceeds that of the receive antennas N at the base station (BS), namely, in the challenging scenario of rank-deficient systems. We demonstrate that the iterative decoding convergence of this two-stage system may be improved by incorporating a unity rate code (URC) having an infinite impulse response, which improves the efficiency of the extrinsic information exchange. Although this results in a slightly more complex three-stage system architecture, it allows us to use a low-complexity SD having a significantly reduced candidate list size N_{cand}. Alternatively, a reduced signal-to-noise ratio (SNR) is required. For example, given a target bit error ratio (BER) of 10^{-5} and $N_{\mathrm{cand}} = 32$ for the SD, the three-stage receiver is capable of achieving a performance gain of 2.5 dB over its two-stage counterpart in a rank-deficient SDMA/OFDM 4-quadratic-amplitude modulation (4-QAM) system supporting $U = 8$ cochannel users and employing $N = 4$ receive antennas at the BS, namely, in an (8×4) system. For the sake of further enhancing the three-stage concatenated receiver, the proposed iterative center-shifting SD scheme and the irregular convolutional codes (IrCCs) are intrinsically amalgamated, which leads to an additional performance gain of 2 dB.**

***Index Terms*—Irregular convolutional coding, SDMA–OFDM, spatial division multiple access, sphere decoding, three-stage concatenated coding.**

Manuscript received February 27, 2008; revised July 22, 2008, September 14, 2008, and September 21, 2008. First published October 31, 2008; current version published April 22, 2009. The review of this paper was coordinated by Prof. H. Nguyen.

The authors are with the School of Electronics and Computer Science (ECS), University of Southampton, SO17 1BJ, Southampton, U.K. (e-mail: lw05r@ecs.soton.ac.uk.; lx04r@ecs.soton.ac.uk.; sqc@ecs.soton.ac.uk.; lh@ecs.soton.ac.uk).

Digital Object Identifier 10.1109/TVT.2008.2007465

I. Motivation

In an uplink spatial-division multiple access (SDMA) system [1], the data streams of multiple users that share the same time/frequency channel are superimposed at the input of the receiver and recovered with the aid of their unique user-specific spatial signature at the base station (BS), which results in a potentially significant increase in spectral efficiency. However, to achieve the optimum BER performance in an SDMA system, the classic maximum likelihood (ML) detector conducts an exhaustive search over the entire $\mathcal{M}_c^U$-element search space of the U-user uplink scheme employing $\mathcal{M}_c$-ary modulation. Hence, the ML detector exhibits a potentially excessive computational complexity. It was shown in [2]–[4] that sphere detection (SD) is capable of attaining a near-ML performance at a significantly reduced complexity. Motivated by the SD proposals in [2]–[5], the researchers have recently proposed diverse further complexity reduction schemes, such as, for example, those in [3] and [6]–[8]. Nonetheless, their complexity may still become potentially unaffordable in high-throughput uplink systems invoking high-order modulation schemes and/or supporting a high number of users. This complexity problem may further be aggravated in rank-deficient systems, where the number of users exceeds that of the receiver antennas at the BS. Recently, the idea of choosing the hard-decision ML symbol point as the list sphere detection's search center was proposed by Boutros *et al.* [9], which has the advantage of requiring a modest list size in the context of depth-first SDs.

Against this background, the novelty of this paper is outlined as follows. 1) We propose the center-shifting philosophy for the SD, which generalizes the scheme in [9], which leads to a potentially considerable reduction in the overall complexity imposed by the SD-aided iterative turbo receiver as a benefit of its substantially reduced candidate list. 2) Motivated by the three-stage single-input–single-output (SISO) turbo equalizer in [10], we significantly improve the performance of the conventional two-stage SD-aided turbo receiver. We achieve this improvement by intrinsically amalgamating the SD with the decoder of a unity rate code (URC) having an infinite impulse response (IIR), both of which are embedded in a channel-coded SDMA orthogonal frequency-division multiplexing (OFDM) transceiver, hence creating a powerful three-stage serially concatenated scheme. 3) For the sake of achieving a near-capacity performance, irregular convolutional codes (IrCCs) are used as the outer code for the proposed iterative center-shifting SD-aided three-stage system. In conclusion, we will demonstrate that at a target BER of 10^{-5}, a performance gain of as high as 4.5 dB is attained by our proposed system by using an SD that relies on a low-complexity candidate list size of $N_{\text{cand}} = 32$ in comparison to its two-stage counterpart in the challenging scenario of an (8×4)-element rank-deficient 4-quadratic-amplitude modulation (4-QAM) SDMA–OFDM uplink system.

The rest of this paper is organized as follows. Section II describes the system model of our uplink SDMA–OFDM system. The proposed K-best SD-aided three-stage transceiver is described in Section III, followed by our EXIT chart analysis [11] in Section IV, where the Monte Carlo simulation results are also provided. Finally, in Section V, we offer our conclusions.

II. System Model

Since the OFDM [1] has been developed into a promising candidate for next-generation wideband digital communication, which is capable of coping with the severe channel conditions imposed by the multipath-induced frequency-selective fading, we intend to investigate our proposed scheme in the scenario of an uplink SDMA–OFDM system. Furthermore, due to the fact that a nondispersive fading is encountered by each subcarrier, our scheme is equally applicable to single-carrier narrowband modems. Hence, let us consider the following generic narrowband system model constructed for SDMA systems supporting U number of single-antenna-aided users and having N number of receive antennas at the BS [1] for a specific subcarrier

$$\mathbf{y} = \mathbf{H}\mathbf{s} + \mathbf{w} \tag{1}$$

where $\mathbf{y} \in \mathbb{C}^{N\times 1}$, $\mathbf{s} \in \mathbb{C}^{U\times 1}$, and $\mathbf{w} \in \mathbb{C}^{N\times 1}$ denote the received signal and the transmitted signal vector as well as the additive white Gaussian noise (AWGN) sample vector, respectively. Moreover, the frequency-domain channel transfer factor matrix $\mathbf{H}$ is a $(N \times U)$-dimensional independent and identically distributed (i.i.d.) zero-mean unit-variance complex Gaussian matrix, which is perfectly known to the receiver, with each column representing the unique spatial signature of the corresponding user [1]. Furthermore, the AWGN noise w_n encountered at the nth receive antenna element exhibits a zero-mean and a variance of σ_w^2.

III. Sphere-Detection-Aided Three-Stage Iterative Receiver

A. K-Best List Sphere Detection

The well-known ML solution may be formulated as [1]

$$\hat{\mathbf{s}}_{\text{ML}} = arg \min_{\check{\mathbf{s}} \in M_c^U} \|\mathbf{y} - \mathbf{H}\check{\mathbf{s}}\|_2^2 \tag{2}$$

where M_c is the number of modulated symbol points in the constellation, and U is the number of users supported by the system. Under the assumption of constant-modulus-constellation modulation schemes, such as BPSK and 4-QAM, with the aid of the MMSE solution of $\hat{\mathbf{x}}_c = (\mathbf{H}^H\mathbf{H} + \sigma_w^2\mathbf{I})\mathbf{H}^H\mathbf{y}$ and the Cholesky factorization of the matrix $(\mathbf{H}^H\mathbf{H} + \sigma_w^2\mathbf{I})$ [2], the ML solution of (2) may be transformed into [12]

$$\hat{\mathbf{s}}_{\text{ML}} = arg \min_{\check{\mathbf{s}} \in M_c^U} (\hat{\mathbf{s}} - \hat{\mathbf{x}}_c)^H \mathbf{U}^H \mathbf{U} (\hat{\mathbf{s}} - \hat{\mathbf{x}}_c) \tag{3}$$

$$= arg \min_{\check{\mathbf{s}} \in M_c^U} \sum_{i=1}^{M} \underbrace{u_{ii}^2 [\check{s}_i - \hat{x}_i + \sum_{j=i+1}^{M} \frac{u_{ij}}{u_{ii}} (\check{s}_j - \hat{x}_j)]^2}_{\phi} \tag{4}$$

where $\mathbf{U}$ is a $(U \times U)$-element upper triangular matrix that satisfies $\mathbf{U}^H\mathbf{U} = \mathbf{H}^H\mathbf{H} + \sigma_w^2\mathbf{I}_C$. For the K-best SD [4], instead of considering all the legitimate bit combinations at each search tree level, we only retain a fixed number of K decision states also referred to as decision nodes, namely, those that have the smallest accumulated *Partial Euclidean Distances* (PEDs) from the SD's initial search center constituted, for example, by the classic MMSE solution [1], where the PEDs correspond to the term ϕ in (4). The corresponding search tree was exemplified in [13]. Hence, after the search reaches the tree leaf level, a candidate list $\mathcal{L}$ is generated, which contains $N_{\text{cand}} = K$ number of $(\log_2 M_c \cdot U)$-length bit candidate vectors, which are then used for the *extrinsic* log likelihood ratio (LLR) calculation by the iterative SISO receiver [3].

B. Center-Shifting Theory for SDs

According to (4), when using list sphere detection, the maximum *a posteriori* (MAP) solution can be found by generating a reduced-size candidate list within a shrinked search hypersphere centered around

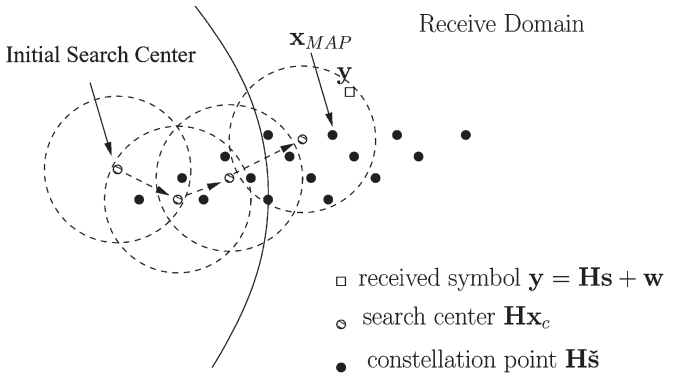

Fig. 1. Geometric representation of the iterative center-shifting SD scheme.

the MMSE solution by choosing an appropriate value for K. During our investigations, we realized that it would be desirable to set the SD's search center to a multiuser signal constellation point, which may be expected to be closer to the real MAP solution than the MMSE solution because this would allow us to reduce the SD's search space and hence its complexity. The benefits of choosing a more accurate search center are clearly illustrated in Fig. 1. Indeed, when the faded and noise-contaminated received signal $\mathbf{y}$ is far from any of the legitimate channel-rotated composite multistream constellation points, the conventional SD has to carry out the search within a large hyperspherical search space centered at $\mathbf{y}$ to maintain a near-MAP performance. Hence, this solution may potentially exhibit an excessive complexity. When the center $\mathbf{Hx}_c$ of the sphere is chosen to be an increasingly accurate symbol point during the consecutive center-updating operations in Fig. 1, the search space quantified by the value of K in the context of K-best SD can dramatically be reduced. Accordingly, when the center is shifted in the vicinity of the real MAP solution, only the constellation points with a high likelihood are taken into account. Hence, it is plausible that the closer the search center to the real MAP solution, the lower the computational efforts required to achieve a near-MAP performance.

Furthermore, the search itself and the search center calculation can independently be carried out. Thus, the search center can be obtained not only by the conventional MMSE detection scheme but also by more sophisticated detection regimes. For example, the SD scheme in [9] is centered at the hard-decision ML solution obtained by invoking the hard-input–hard-output (HIHO) SD prior to activating the SISO list sphere decoder (LSD). Our proposed center-shifting scheme turns the SD into a high-flexibility detector, which can readily be combined with other well-established linear or nonlinear detectors. As a result, the affordable computational complexity can flexibly be split between the center calculation phase and the search phase. It is also plausible that an improved performance versus complexity tradeoff emerges if the search center calculation is regularly updated before further triangularization and PED calculation are carried out.

C. URC-Assisted Three-Stage Iterative Receiver With Iterative Center-Shifting Sphere-Detection

Based on the observations outlined in Section III-B, we can infer that the center-shifting scheme applied for the SD may effectively be employed in an iterative detection-aided channel-coded system since the process of obtaining a more accurate search center is further aided by the channel decoder, which substantially contributes toward the total error correction capability of the iterative receiver. Moreover, in comparison to the scheme proposed in [9], where the search center is only updated once at the very beginning to the hard-decision ML solution by invoking the HIHO SD prior to activating the SISO LSD, we formulate the center-shifting SD-aided receiver design principles as follows.

1) The search center calculation is based on the soft bit information provided by the channel decoder, namely, the *extrinsic* LLR values.
2) The search center update can be carried out in a more flexible manner by activating the proposed center-shifting scheme whenever the system needs its employment during the iterative detection process to maximize the achievable iterative gain.
3) The search center update is flexible since it may be carried out by any of the well-known linear or nonlinear detection techniques. We employed the soft interference cancellation MMSE (SIC-MMSE) algorithm in [14] to calculate the search center based on the *a priori* information provided by the channel decoder.[1]

Fig. 2 depicts the system model of the SD-aided three-stage serially concatenated transceiver in the context of an uplink SDMA/OFDM system. For a specific user/mobile station (MS), a block of L information bits u_1 is first encoded by the convolutional channel encoder I to generate the coded bits c_1, which are interleaved by the interleaver Π_1 in Fig. 2. Then, the resultant permuted bits u_2 are fed through the URC encoder II and the interleaver Π_2, which yields the interleaved double-encoded bits u_3 that are delivered to the bit-to-symbol modulator/mapper in Fig. 2. Note that the labels u and c represent the uncoded and coded bits, respectively, which correspond to the specific module indicated by the subscript. For example, u_2 and c_2 denote the uncoded and coded bits at the input and output of the URC encoder II in Fig. 2, respectively. At the receiver in Fig. 2, which is constituted by three modules, namely, the SD, the URC decoder II, and the channel decoder I, the extrinsic information is exchanged among the blocks in a number of consecutive iterations. Specifically, as shown in Fig. 2, $A(\cdot)$ represents the *a priori* information expressed in terms of the LLRs, whereas $E(\cdot)$ denotes the corresponding *extrinsic* information. Hence, the URC decoder generates two *extrinsic* outputs by processing two *a priori* inputs delivered from both the SD and the channel decoder I. After completing the last iteration, the estimates $\hat{u}_1$ of the original transmitted information bit u_1 are produced by the channel decoder I. On the other hand, if the aforementioned SIC-MMSE-aided center-shifting scheme is employed, there will be an additional search center update block between the SD and the URC decoder II. To be specific, the *a priori* LLRs are not only directly fed to the SD but also delivered to the center calculation functional block in Fig. 2 for updating the search center $\hat{\mathbf{x}}_c$ of the SD. Hence, in contrast to the conventional SD dispensing with the center-shifting scheme, every time the search center $\hat{\mathbf{x}}_c$ is updated, the SD is required to regenerate the candidate list, which is used to calculate the *extrinsic* LLRs delivered to the outer channel decoder in Fig. 2.

IV. EXIT Chart Analysis and Simulation Results

A. EXIT Chart Analysis

The EXIT charts were proposed by ten Brink [11] for analyzing the convergence characteristics of the turbo codes as a convenient visualization technique. This technique computes the mutual information (MI) of the output extrinsic and input *a priori* components that correspond to the associated bits for each of the iterative SISO blocks. In line with the notation used in [10], we denote the MI between the *a priori* value $A(b)$ and the bit b as $I_{A(b)}$, whereas the

[1]Every time the search center $\mathbf{x}_c$ in the transmit domain is updated by exploiting the *a priori* LLRs provided by the outer channel decoder using the SIC-MMSE algorithm, the SD is required to regenerate the candidate list, which is used to calculate the *extrinsic* LLRs delivered to the outer channel decoder.

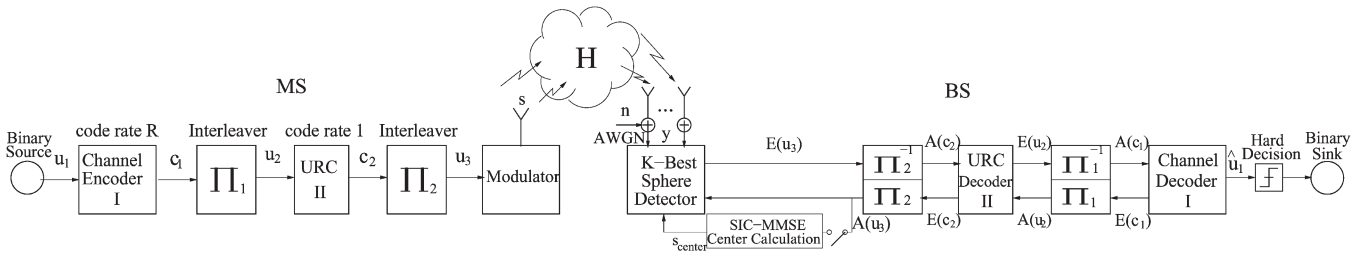

Fig. 2. Three-stage serially concatenated receiver architecture of the SIC-MMSE-aided iterative center-shifting K-best SD scheme.

MI between the *extrinsic* value $E(b)$ and the bit b is denoted by $I_{E(b)}$. Hence, the MIs of the two outputs of the URC decoder, namely, $I_{E(u_2)}$ and $I_{E(c_2)}$, are functions of the two *a priori* MI inputs, namely, of $I_{A(u_2)}$ and $I_{A(c_2)}$. To avoid the cumbersome 3-D EXIT chart representation [10], which is needed to exhaustively represent the EXIT characteristics of the double-input–double-output URC decoder, we now view the SD and the URC decoder II in Fig. 2 as a joint SISO module that delivers the *extrinsic* information $E(u_3)$ to the decoder I by exploiting the single *a priori* information input $A(u_3)$ provided by decoder I in Fig. 2. Thus, a single 2-D EXIT chart is sufficient for characterizing each of the concatenated SISO modules of the three-stage receiver, namely, the combined module constituted by the SD and the URC decoder II, as well as the channel decoder I. Upon denoting the EXIT function by $T[\cdot,\cdot]$, we have the corresponding EXIT functions expressed as

$$I_{E(u_2)} = T_{u_2}\left[I_{A(u_2)}, E_b/N_0\right] \tag{5}$$

for the joint SD and URC decoder module as well as

$$I_{E(c_1)} = T_{c_1}\left[I_{A(c_1)}\right] \tag{6}$$

for the channel decoder I. In our forthcoming discourse, we simply refer to the aforementioned combined module as the *inner decoder*, whereas we denote the channel decoder I as the *outer decoder* in the context of the three-stage receiver shown in Fig. 2. Similarly, we also refer to the SD as the inner decoder and to the channel decoder as the outer decoder in the scenario of the conventional two-stage receiver dispensing with the URC decoder.

In comparison to the EXIT curves of the concatenated inner and outer decoders of the two-stage iterative receiver, Fig. 3 depicts those of the combined inner decoder and the outer decoder of the three-stage receiver in Fig. 2 at the signal-to-noise ratio SNR $= 8$ dB in the highly rank-deficient scenario of (8×4)-element SDMA/OFDM systems[2]both with and without our proposed SIC-MMSE-aided channel-coded iterative center-shifting scheme discussed in Sections III-B and C. In addition, Fig. 3 also plots two EXIT curves that correspond to two distinct outer decoders. Specifically, the continuous curve marked by crosses is the EXIT curve of the recursive systematic convolutional code (RSC), and the continuous line marked by dots corresponds to the IrCC [15], [16], which will be discussed in Section IV-B. The system parameters used in our simulations are provided in Table I. As observed in Fig. 3, in the absence of URC encoding/decoding, the maximum achievable iterative gain of the traditional two-stage receiver having an SD using $N_{\text{cand}} = 1024$ detection candidates for achieving a near-MAP performance is rather limited. This is because the EXIT curve of the inner decoder has a relatively low I_E value at $I_A = 1$, which is in contrast to the corresponding EXIT curve of its three-stage counterpart having an ending point of $(I_A, I_E) = (1, 1)$ in

[2]This rank-deficient scenario is considered because unless the system's admission control prevents additional uplink users from joining the system, this scenario may realistically be encountered.

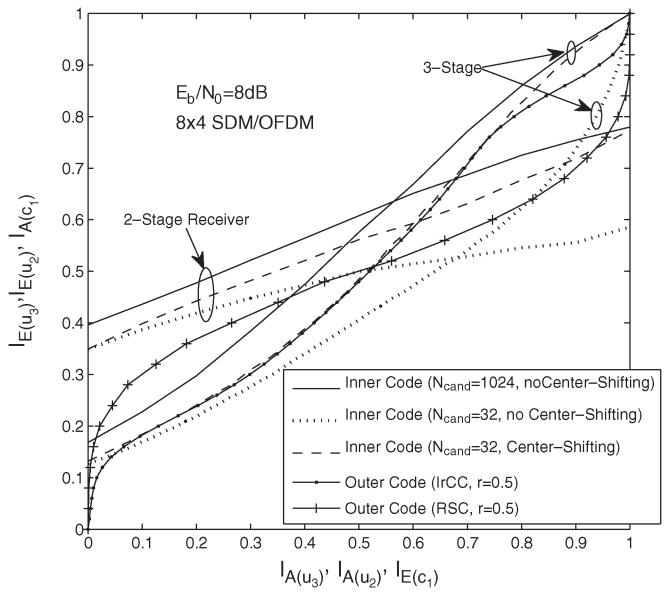

Fig. 3. EXIT charts of the URC-aided three-stage receiver in the scenario of 8×4-element SDMA/OFDM system at $E_b/N_0 = 8$ dB.

TABLE I
SUMMARY OF THE SYSTEM PARAMETERS FOR THE K-BEST SD-AIDED CODED SDMA–OFDM SYSTEM

System Parameters	Choice
System	SDMA/OFDM
No. of Sub-Carriers	1024
Modulation	4-QAM
No. of Transmit Antenna	8
No. of Receive Antenna	4
Block Length	102400
CIR Tap Fading	OFDM symbol invariant
Channel Estimation	Ideal
Detector/MAP	K-Best List-SD
List Length $\mathcal{N}_{cand}$	$=K$
Channel Encoder I	Half-Rate RSC (2,1,3) Generator Polynomials $(5/7)$
	or Half-Rate IrCC
URC Encoder II	Generator Polynomials $1/(1+D)$
Max No. of Detection Iterations	10

Fig. 3. To considerably reduce the excessive computational complexity imposed by the SD in such a high-throughput heavily rank-deficient system, we significantly reduce the detection candidate list size to $N_{\text{cand}} = 32$. As a price, the maximum achievable throughput of both the two-stage and the three-stage receivers is significantly decreased. The achievable throughput may be approximated by the area under the inner code's EXIT curve in Fig. 3 under the assumption of having a uniformly distributed discrete channel input [17]. However, as a benefit of employing URC encoding/decoding, the ending point of the inner

code's EXIT curve in the three-stage receiver remains $(I_A, I_E) = (1, 1)$, whereas that of the two-stage receiver drops from (1, 0.77) to (1, 0.59), which results in an even lower maximum achievable iterative gain. Therefore, as long as there is an open tunnel between the EXIT curves of the inner and outer decoders, the three-stage concatenated system is capable of achieving an iterative decoding convergence to the $(I_A, I_E) = (1, 1)$ point, hence achieving an infinitesimally low BER despite employing a significantly reduced candidate list size N_{cand}. By contrast, the inner code's EXIT curve of its two-stage counterpart is unable to reach the point of convergence at (1, 1) since it intersects with the outer code's EXIT curve, which implies that residual errors persist regardless of the complexity invested. More explicitly, despite using a high number of iterations as well as the high "per-iteration" SD complexity quantified in terms of its candidate list size, the two-stage scheme is outperformed by the three-stage arrangement.

Nonetheless, we also observe from Fig. 3 that the inner code's EXIT curve in the two-stage receiver emerges from a higher starting point at $I_A = 0$ than that of its three-stage counterpart. This leads to a potentially lower BER at relatively low SNRs, where I_A is also low, although the exact behavior is determined by the SD complexity as well as the SNR. In other words, although the employment of the URC encoder/decoder pair at the transmitter/receiver is capable of eliminating the EXIT curve intercept point, an open EXIT tunnel can only be formed if the value of $K = N_{\text{cand}}$ as well as that of the SNR is sufficiently high.

The reason why a URC will make the slope of the EXIT chart curve steeper, hence resulting in a lower error floor and a higher BER waterfall threshold, can be interpreted as follows. Since the URC has an IIR due to its recursive coding structure, the corresponding EXIT chart curve is capable of reaching the highest point of perfect convergence to an infinitesimally low BER (1, 1) provided that the interleaver length is sufficiently large [18]. On the other hand, since the URC decoder employs the MAP decoding scheme, the extrinsic probability computed at the output of the URC decoder contains the same amount of information as the sequence at the input of the URC decoder. In other words, the area under the inner EXIT curve remains unchanged regardless of the employment of the URC [19], [20]. Hence, a higher ending point of the EXIT curve leads to having a lower starting point, which implies a steeper slope of the EXIT curve.

On the other hand, observe in Fig. 3 that the employment of our proposed SIC-MMSE-aided center-shifting-assisted SD is capable of considerably counteracting the potentially detrimental effects of using a limited detection candidate list size N_{cand}. This is because as a benefit of the center-shifting scheme, the area under the inner code's EXIT curve of both the two-stage and the three-stage receivers approaches that of the MAP detector-assisted system using an SD having $N_{\text{cand}} = 1024$, as observed in Fig. 3. Observe, however, in Fig. 3 that the three-stage system only requires $N_{\text{cand}} = 32$ detection candidates for matching this performance.

B. Design of Irregular Convolutional Codes

The so-called IrCCs [15], [16] proposed by Tüchler and Hagenauer appropriately encode the chosen "fractions" of the input stream by using punctured constituent convolutional codes that have different code rates. The appropriate "fractions" are specifically designed with the aid of EXIT charts for the sake of improving the convergence behavior of the iteratively decoded systems. Thus, with the aid of IrCCs, we are able to solve the mismatch between the EXIT curve of the inner decoder in the three-stage receiver and the EXIT curve of the RSC (2, 1, 3) code marked by crosses in Fig. 3. Our goal is to achieve an improved convergence behavior for the three-stage concatenated system by minimizing the area between the EXIT curve of the amalgamated two-compound inner code and that of the outer code. The resultant EXIT curve of the optimized IrCC having a code rate of 0.5 is represented by the dotted line in Fig. 3. Hence, a narrow but still open EXIT chart tunnel is created, which implies having a near-capacity performance attained at the cost of a potentially high number of decoding iterations, although the "per-iteration" complexity may be low.

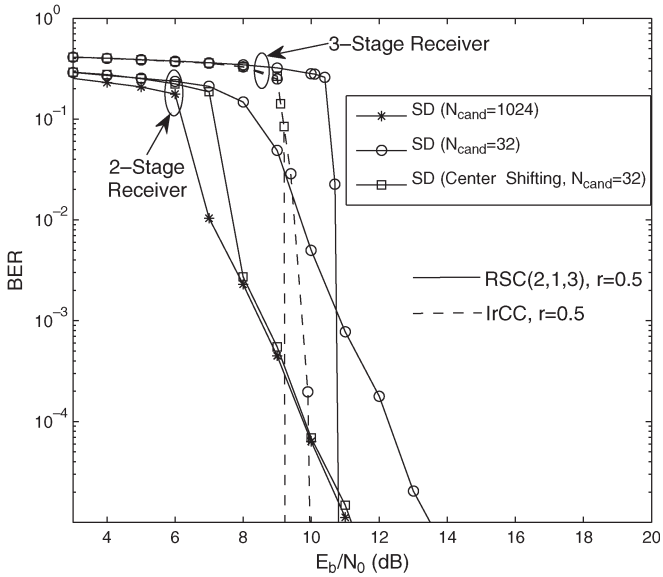

Fig. 4. BER performance comparison between the three-stage iterative receiver using the K-best SD and its two-stage counterpart in the scenario of an (8×4)-element SDMA/OFDM system.

C. Simulation Results and Discussion

1) BER Performance: Monte Carlo simulations were performed for characterizing both the decoding convergence prediction in Section IV-A and the IrCC design in Section IV-B in the high-throughput overloaded (8×4) SDMA/OFDM system. As our benchmarker system, the half-rate RSC(2, 1, 3) code's EXIT curve that is marked by crosses in Fig. 3 is employed as the outer code of the traditional two-stage receiver. As our proposed scheme, the half-rate IrCC that corresponds to the EXIT curve represented by the dotted line in Fig. 3 is used as the outer code in the URC-assisted three-stage receiver. Fig. 4 compares the BER performance of both systems, where we can see that at relatively high SNRs both of the three-stage concatenated receivers—namely, that using the SD employing the classic RSC code as well as that employing the optimized IrCC code—are capable of outperforming the traditional two-stage receiver equipped with the SD. Specifically, given a target BER of 10^{-5}, a performance gain of 2.5 dB can be attained by the three-stage receiver over its two-stage counterpart when both of them employ the SD $(N_{\text{cand}} = 32)$ and the regular RSC. Remarkably, when amalgamated with the URC encoder/decoder, the three-stage receiver that uses the SD and $N_{\text{cand}} = 32$ becomes capable of outperforming the two-stage receiver by using the high-complexity near-MAP SD having $N_{\text{cand}} = 1024$ provided that the SNR is in excess of about 11 dB. Furthermore, an additional performance gain of 1 dB can be attained by employing the optimized IrCC in comparison to the classic RSC-aided three-stage system. Moreover, to further enhance the achievable performance, when the SIC-MMSE-aided iterative center-shifting SD is invoked, another approximately 1-dB additional performance gain is attained. Consequently, as observed in Fig. 4, given a target BER of 10^{-5}, the overall performance gains of 4.5

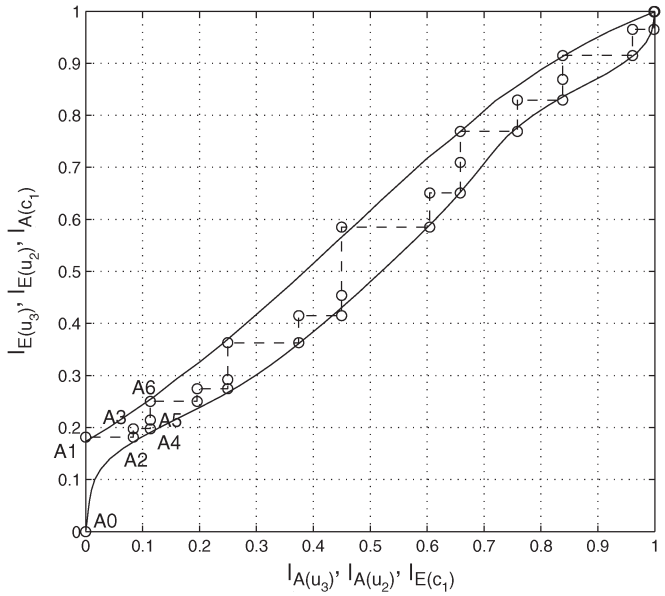

Fig. 5. EXIT charts and recorded decoding trajectory for the three-stage receiver using IrCC at $E_b/N_0 = 9.5$ dB in the scenario of (8×4)-element SDMA/OFDM system.

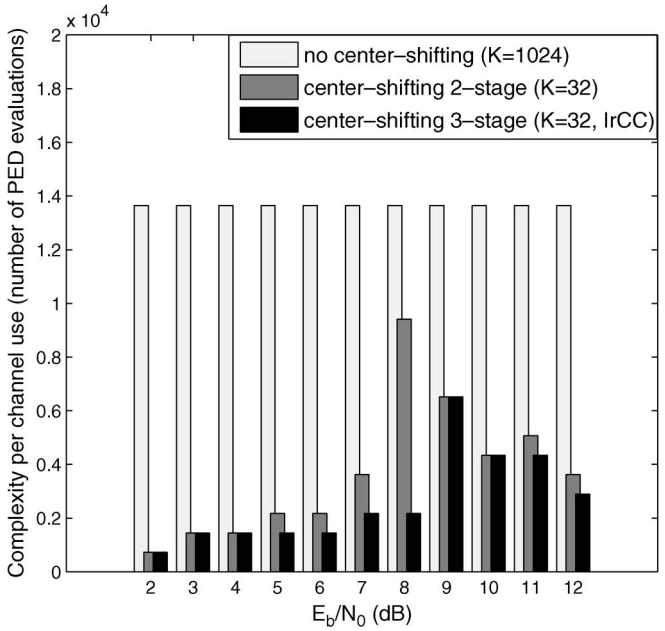

Fig. 6. Complexity reduction achieved by the three-stage iterative receiver using the K-best SD over its two-stage counterpart as well as the non–center-shifting SD-aided two-stage benchmark receiver in the scenario of an (8×4)-element SDMA/OFDM system.

and 2 dB are attained by our proposed system in comparison to its SD-aided $(N_{\text{cand}} = 32)$ and SD-assisted $(N_{\text{cand}} = 1024)$ two-stage counterparts, respectively.

In line with the EXIT-chart-based predictions in Fig. 3, a sharp BER improvement is achieved by the three-stage receiver, as shown in Fig. 4, since the EXIT curve of the inner code will rise above that of the outer code for SNRs in excess of a certain level, which results in a consistently open EXIT tunnel leading to the point of convergence at (1, 1), which is exemplified in Fig. 5 by the curve recorded at SNR $= 9.5$ dB when using the half-rate IrCC as the outer code. In addition, shown in Fig. 5 is the staircase-shaped decoding trajectory that evolves through the open tunnel to the point of convergence at (1, 1), as recorded during our Monte Carlo simulations. The activation order of the three SISO modules used is [3 2 1 2 1 2], where the integers represent the index (I) of the three SISO modules. Specifically, $I = 3$ denotes the SD, $I = 2$ represents the URC decoder II, and $I = 1$ denotes the channel decoder I in Fig. 2. Hence, the vertical coordinates of the points A_1, A_3, and A_5 in Fig. 5 quantify the $I_{E(u_2)}$ value measured at the output of the URC decoder II corresponding to its three successive activations during the first iteration, respectively, whereas the segments between A_1 and A_2 as well as between A_3 and A_4 represent two successive activations of the channel decoder I during the first iteration, respectively. The segment between A_5 and A_6 in Fig. 5 denotes the beginning of a new iteration associated with similar decoding activations.

2) Computational Complexity: Fig. 6 depicts the computational complexity—which is quantified in terms of the number of PED evaluations that correspond to the term ϕ in (4)—imposed by the SD versus E_b/N_0 for the aforementioned receivers. Note that the computational complexity imposed by the K-best SD dispensing with the center-shifting scheme remains constant for both two-stage and three-stage receivers regardless of the SNR and the number of iterations under the assumption that the buffer size is sufficiently large to store the resultant candidate list $\mathcal{L}$, which is generated by the SD just once during the first iteration between the SD and the channel decoder. On the other hand, as mentioned in Section III-C, every time the search center $\mathbf{x}_c$ in the transmit domain is updated, the SD is required to regenerate the candidate list. However, as observed in Fig. 6, the candidate list size N_{cand} can substantially be reduced with the aid of the center-shifting scheme; hence, the resultant overall complexity imposed by the SD becomes significantly lower than that of the receiver using no center shifting. Explicitly, the candidate list generation complexity of the SIC-MMSE center-shifting-aided two-stage receiver is well below that of the receiver using no center shifting right across the SNR range spanning from 2 to 12 dB. This statement is valid if our aim is to achieve the near-MAP BER performance quantified in Fig. 4, which can be attained by having $K = N_{\text{cand}} = 1024$ for the system operating without the center-shifting scheme or by setting $K = N_{\text{cand}} = 32$ in the presence of the center-shifting scheme. The number of PED evaluations carried out per channel use by the system dispensing with the center-shifting scheme remains as high as 13 652 regardless of the SNR and the number of iterations. On the other hand, in the presence of the center-shifting scheme, the candidate list has to be regenerated at each iteration, but nonetheless, the total complexity imposed is substantially reduced. We can also observe from Fig. 6 that the center-shifting K-best SD employed by the URC-aided three-stage system imposes a computational complexity, which is even below that of its center-shifting-aided two-stage counterpart while achieving a performance gain of 2 dB for a target BER of 10^{-5}, as shown in Fig. 4. Hence, the significant complexity reduction facilitated by the proposed SD scheme in the context of the three-stage receiver outweighs the relatively small additional complexity cost imposed by the URC, which only employs a two-state trellis, which leads to an overall reduced complexity. Furthermore, in addition to the complexity reduction achieved by the proposed scheme, another benefit is the attainable memory reduction since there is no need to store the resultant candidate list for the forthcoming iterations. As a result, the memory size required can substantially be reduced by having a significantly reduced value of K.

V. Conclusion

An SD-aided three-stage scheme has been proposed, which is capable of achieving a substantial BER performance gain in comparison

to the classic two-stage scheme, provided that the SNR is sufficiently high. For example, given a target BER of 10^{-5}, the three-stage receiver using SD ($N_{\text{cand}} = 32$) is capable of achieving a performance gain of 2.5 dB over its two-stage counterpart in an uplink (8×4) SDMA/OFDM 4-QAM system. Furthermore, an additional 2-dB performance gain can be attained with the aid of the novel center-shifting-based SD amalgamated with an IrCC.

REFERENCES

[1] L. Hanzo, M. Munster, B. J. Choi, and T. Keller, *OFDM and MC-CDMA for Broadband Multi-User Communications, WLANs and Broadcasting*. Piscataway, NJ: IEEE Press, 2003.

[2] E. Viterbo and J. Boutros, "A universal lattice code decoder for fading channels," *IEEE Trans. Inf. Theory*, vol. 45, no. 5, pp. 1639–1642, Jul. 1999.

[3] B. M. Hochwald and S. ten Brink, "Achieving near-capacity on a multiple-antenna channel," *IEEE Trans. Commun.*, vol. 51, no. 3, pp. 389–399, Mar. 2003.

[4] K. Wong, C. Tsui, R. S. K. Cheng, and W. Mow, "A VLSI architecture of a K-best lattice decoding algorithm for MIMO channels," in *Proc. IEEE Int. Symp. Circuits Syst.*, May 2002, vol. 3, pp. 273–276.

[5] W. H. Mow, "Maximum likelihood sequence estimation from the lattice viewpoint," *IEEE Trans. Inf. Theory*, vol. 40, no. 5, pp. 1591–1600, Sep. 1994.

[6] A. M. Chan and I. Lee, "A new reduced-complexity sphere decoder for multiple antenna systems," in *Proc. IEEE Int. Conf. Commun.*, Apr./May 2002, vol. 1, pp. 460–464.

[7] A. Wolfgang, J. Akhtman, S. Chen, and L. Hanzo, "Reduced-complexity near-maximum-likelihood detection for decision feedback assisted space–time equalization," *IEEE Trans. Wireless Commun.*, vol. 3, no. 7, pp. 2407–2411, Jul. 2007.

[8] Y. Xie, Q. Li, and C. N. Georghiades, "On some near optimal low complexity detectors for mimo fading channels," *IEEE Trans. Wireless Commun.*, vol. 6, no. 4, pp. 1182–1186, Apr. 2007.

[9] J. Boutros, N. Gresset, L. Brunel, and M. Fossorier, "Soft-input soft-output lattice sphere decoder for linear channels," in *Proc. IEEE Global Telecommun. Conf.*, Dec. 2003, vol. 3, pp. 1583–1587.

[10] J. Wang, S. X. Ng, L. L. Yang, and L. Hanzo, "Combined serially concatenated codes and MMSE equalization: An EXIT chart aided perspective," in *Proc. IEEE Veh. Technol. Conf.—Fall*, Sep. 2006, pp. 1–5.

[11] S. ten Brink, "Convergence behavior of iteratively decoded parallel concatenated codes," *IEEE Trans. Commun.*, vol. 49, no. 10, pp. 1727–1737, Oct. 2001.

[12] T. Cui and C. Tellambura, "An efficient generalized sphere decoder for rank-deficient MIMO systems," *IEEE Commun. Lett.*, vol. 9, no. 5, pp. 423–425, May 2005.

[13] L. Hanzo and T. Keller, *OFDM and MC-CDMA: A Primer*. Hoboken, NJ: Wiley, 2006.

[14] M. Tuchler, A. C. Singer, and R. Koetter, "Minimum mean squared error equalization using *a priori* information," *IEEE Trans. Signal Process.*, vol. 50, no. 3, pp. 673–683, Mar. 2002.

[15] M. Tüchler and J. Hagenauer, "Exit charts of irregular codes," in *Proc. Conf. Inf. Sci. Syst.*, 2002, pp. 20–22. CD-ROM.

[16] M. Tüchler, "Design of serially concatenated systems depending on the block length," *IEEE Trans. Commun.*, vol. 52, no. 2, pp. 209–218, Feb. 2004.

[17] A. Ashikhmin, G. Kramer, and S. ten Brink, "Extrinsic information transfer functions: Model and erasure channel properties," *IEEE Trans. Inf. Theory*, vol. 50, no. 11, pp. 2657–2673, Nov. 2004.

[18] J. Kliewer, S. X. Ng, and L. Hanzo, "Efficient computation of exit functions for nonbinary iterative decoding," *IEEE Trans. Commun.*, vol. 54, no. 12, pp. 2133–2136, Dec. 2006.

[19] J. Kliewer, A. Huebner, and D. J. Costello, "On the achievable extrinsic information of inner decoders in serial concatenation," in *Proc. IEEE Int. Symp. Inf. Theory*, Seattle, WA, Jul. 2006, pp. 2680–2684.

[20] S. X. Ng, J. Wang, and L. Hanzo, "Unveiling near-capacity code design: The realization of Shannon's communication theory for MIMO channels," in *Proc. IEEE Int. Conf. Commun.*, May 2008, pp. 1415–1419.

On the Optimality of the Null Subcarrier Placement for Blind Carrier Offset Estimation in OFDM Systems

Yan Wu, *Student Member, IEEE*, Samir Attallah, *Senior Member, IEEE*, and J. W. M. Bergmans, *Senior Member, IEEE*

***Abstract*—Liu and Tureli proposed a blind carrier frequency offset (CFO) estimation method for orthogonal frequency-division multiplexing (OFDM) systems, making use of null subcarriers. The optimal subcarrier placement that minimizes the Cramer–Rao bound (CRB) of the CFO estimation was reported by Ghogho *et al.* In this paper, we study the optimality of the null subcarrier placement from another perspective. We first show that the SNR of the CFO estimation using null subcarriers is a function of the null subcarrier placement. We then formulate the CFO-SNR optimization for the null subcarrier placement as a convex optimization problem for small CFO values and derive the optimal placement when the number of subcarriers is a multiple of the number of null subcarriers. In addition, we show that the SNR-optimal null subcarrier placement also minimizes the theoretical mean square error in the high SNR region. When the number of subcarriers is not a multiple of the number of null subcarriers, we propose a heuristic method for the null subcarrier placement that still achieves good performance in the CFO estimation. We also discuss the optimality of the null subcarrier placement in practical OFDM systems, where guard bands are required at both ends of the spectrum.**

***Index Terms*—Blind carrier offset estimation, convex optimization, orthogonal frequency-division multiplexing (OFDM).**

I. INTRODUCTION

Orthogonal frequency-division multiplexing (OFDM) is known to be more sensitive to carrier frequency offset (CFO). For an OFDM system with CFO, we can write the received time-domain signal in the following form [1]:

$$\mathbf{y}^m = \mathbf{E}\mathbf{W}_P\mathbf{H}^m\mathbf{s}^m e^{j2\pi\phi_0(m-1)(1+N_g/N)} + \mathbf{n}^m. \tag{1}$$

Here, we use superscript m to indicate the OFDM symbol index. $\mathbf{E} = \text{diag}(1, e^{j2\pi\phi_0/N}, \ldots, e^{j2\pi(N-1)\phi_0/N})$ is a diagonal matrix containing CFO ϕ_0, which we assume to be normalized with respect to subcarrier spacing $2\pi/N$. In a practical OFDM system, there are some subcarriers that do not carry any data. They are called null subcarriers, whereas the data-carrying subcarriers are simply called data subcarriers. Let P out of N subcarriers be the data subcarriers. Then, $\mathbf{W}_P$ is an $N \times P$ submatrix that is obtained from the $N \times N$ inverse discrete Fourier transform (DFT) matrix $\mathbf{W}_N$. $\mathbf{H}^m$ is a diagonal matrix containing the channel frequency response, $\mathbf{s}^m$ is a $P \times 1$ vector containing the transmitted data in the mth OFDM symbol, N_g denotes the length of the cyclic prefix, and $\mathbf{n}^m$ is an additive white Gaussian noise (AWGN) vector.

Manuscript received September 30, 2007; revised April 11, 2008. First published September 12, 2008; current version published April 22, 2009. The review of this paper was coordinated by Prof. H.-C. Wu.

Y. Wu is with the Signal Processing Systems Group, PT 3.27, Department of Electrical Engineering, Technische Universiteit Eindhoven, 5600 MB Eindhoven, The Netherlands (e-mail: y.w.wu@tue.nl).

S. Attallah is with the School of Science and Technology, SIM University, Singapore 599491 (e-mail: samir@unisim.edu.sg).

J. W. M. Bergmans is with the Signal Processing Systems Group, PT 3.06, Department of Electrical Engineering, Technische Universiteit Eindhoven, 5600 MB Eindhoven, The Netherlands (e-mail: J.W.M.Bergmans@tue.nl).

Color versions of one or more of the figures in this paper are available online at http://ieeexplore.ieee.org.

Digital Object Identifier 10.1109/TVT.2008.2005574